Reinvestigation of the synthesis and evaluation of [*N*-methyl-^{11}C] vorozole, a radiotracer targeting cytochrome P450 aromatase

Sung Won Kim[a],*, Anat Biegon[a], Zachary E. Katsamanis[a], Carolin W. Ehrlich[b],
Jacob M. Hooker[a], Colleen Shea[a], Lisa Muench[c], Youwen Xu[a], Payton King[a],
Pauline Carter[a], David L. Alexoff[a], Joanna S. Fowler[a,d,e]

[a]*Medical Department, Brookhaven National Laboratory, Upton, NY 11973, USA*
[b]*Johannes-Gutenberg Universität Mainz, Institut für Organische Chemie, Duesbergweg 10-14, Mainz, Germany*
[c]*National Institute on Alcoholism and Alcohol Abuse, Bethesda, MD, USA*
[d]*Department of Psychiatry, Mount Sinai School of Medicine, New York, NY, USA*
[e]*Department of Chemistry, State University of New York at Stony Brook, Stony Brook, NY, USA*

Abstract

Introduction: We reinvestigated the synthesis of [*N*-methyl-^{11}C]vorozole, a radiotracer for aromatase, and discovered the presence of an *N*-methyl isomer which was not removed in the original purification method. Herein we report the preparation and positron emission tomography (PET) studies of *pure* [*N*-methyl-^{11}C]vorozole.
Methods: Norvorozole was alkylated with [^{11}C]methyl iodide as previously described and also with unlabeled methyl iodide. A high-performance liquid chromatography (HPLC) method was developed to separate the regioisomers. Nuclear magnetic resonance (NMR) spectroscopy (^{13}C and 2D-nuclear Overhauser effect spectroscopy NMR) was used to identify and assign structures to the *N*-methylated products. Pure [*N*-methyl-^{11}C]vorozole and the contaminating isomer were compared by PET imaging in the baboon.
Results: Methylation of norvorozole resulted in a mixture of isomers (1:1:1 ratio) based on new HPLC analysis using a pentafluorophenylpropyl bonded silica column, in which vorozole coeluted one of its isomers under the original HPLC conditions. Baseline separation of the three labeled isomers was achieved. The N-3 isomer was the contaminant of vorozole, thus correcting the original assignment of isomers. PET studies of *pure* [*N*-methyl-^{11}C]vorozole with and without the contaminating N-3 isomer revealed that only [*N*-methyl-^{11}C]vorozole binds to aromatase. [*N*-methyl-^{11}C]Vorozole accumulated in all brain regions with highest accumulation in the aromatase-rich amygdala and preoptic area. Accumulation was blocked with vorozole and letrozole consistent with reports of some level of aromatase in many brain regions.
Conclusions: The discovery of a contaminating labeled isomer and the development of a method for isolating *pure* [*N*-methyl-^{11}C]vorozole combine to provide a new scientific tool for PET studies of the biology of aromatase and for drug research and development.
© 2009 Elsevier Inc. All rights reserved.

Keywords: [*N*-methyl-^{11}C]vorozole; Positron emission tomography; Breast cancer; Steroid abuse; Estrogen

1. Introduction

Cytochrome P450 aromatase is the last enzyme in estrogen biosynthesis, catalyzing the conversion of androgens to estrogen [1]. It plays a major role in the sexual differentiation of the brain during development [2] and has been implicated in the brain response to injury [3] and in the pathophysiology of Alzheimer's disease [4,5]. The enzyme is highly expressed in liver, steroidogenic organs [6] and specific regions of the brain including the amygdala, the bed nucleus of the stria terminalis, and the preoptic area (POA, anterior hypothalamus) [7]. Moderate or lower levels have been observed in many other brain regions including posterior and lateral hypothalamic nuclei, hippocampus and temporal cortex of rodents, nonhuman primates and man [8].

Aromatase activity can be inhibited reversibly or irreversibly by steroidal as well as nonsteroidal compounds [9]. Aromatase inhibitors are used clinically in the hormonal therapy of breast cancer in women [10]. These drugs are also used by body builders and athletes who abuse anabolic steroids [11-13] as a means of curtailing the estrogenic side effects of excess androgens.

(S)-Vorozole (6-[(S)-(4-chlorophenyl)-1H-1,2,4-triazol-1-ylmethyl]-1-methyl-1H-benzotriazole) (**1**) is a specific and potent nonsteroidal aromatase inhibitor [14,15] originally developed as an antineoplastic agent [16]. It has been labeled with [11]C (half-life=20.4 min) via the N-alkylation of (S)-norvorozole (5-[(S)-(4-chlorophenyl)-1H-1,2,4,-triazol-1-yl)methyl]-1H-benzotriazole) (**4**) with [11C]methyl iodide for PET imaging [17,18] and in vitro studies as a translational research tool for studies of aromatase in brain and peripheral organs for nearly a decade (Scheme 1) [19-22]. The previous study also reported that the N-3 alkylation product ([11]**C-3**) is formed but that it is well separated from [N-methyl-^{11}C]vorozole under the reported HPLC conditions. The two isomers {[N-methyl-^{11}C]vorozole (N-1) and the N-3 isomer} were reported to be produced in a 2:1 ratio. Surprisingly, [N-methyl-^{11}C] vorozole synthesized by the reported procedure showed low target-to-background ratios (i.e., amygdala-to-cerebellum ratio of 1.25) and no reliable blockable uptake in the

preoptic area, despite remarkable metabolic stability in plasma and reasonable brain penetration [18].

We recently reproduced the original synthesis and purification conditions for ^{11}C-labeled vorozole in our laboratory and also encountered low regional specificity and high nonspecific binding in baboon brain imaging studies. After a detailed investigation of the alkylation of norvorozole (**4**) with both ^{12}C and [11C]methyl iodide (Scheme 1), we discovered that the original synthesis produced three regioisomers, not two isomers, and the labeled side product previously reported as the N-3 isomer ([11]**C-3**) was the N-2 isomer ([11]**C-2**). Moreover, under the reported HPLC conditions, the N-3 isomer coeluted with [N-methyl-^{11}C]vorozole (N-1 isomer, [11]**C-1**) and thus affected PET imaging and analysis.

To overcome this, we developed a modified procedure that provides reliable separation of all three methylated products, thus affording *pure* [N-methyl-^{11}C]vorozole ([11]**C-1**) for re-evaluation as an aromatase imaging radiotracer. Herein, we describe the investigation of the alkylation of norvorozole with [^{12}C]methyl iodide and the development of rapid HPLC conditions which achieves baseline separation of the three isomers. In addition, we clarify the previous structural assignments using ^{13}C nuclear magnetic resonance (NMR) spectroscopy and 2D-nuclear Overhauser effect spectroscopy (NOESY). We conclude with
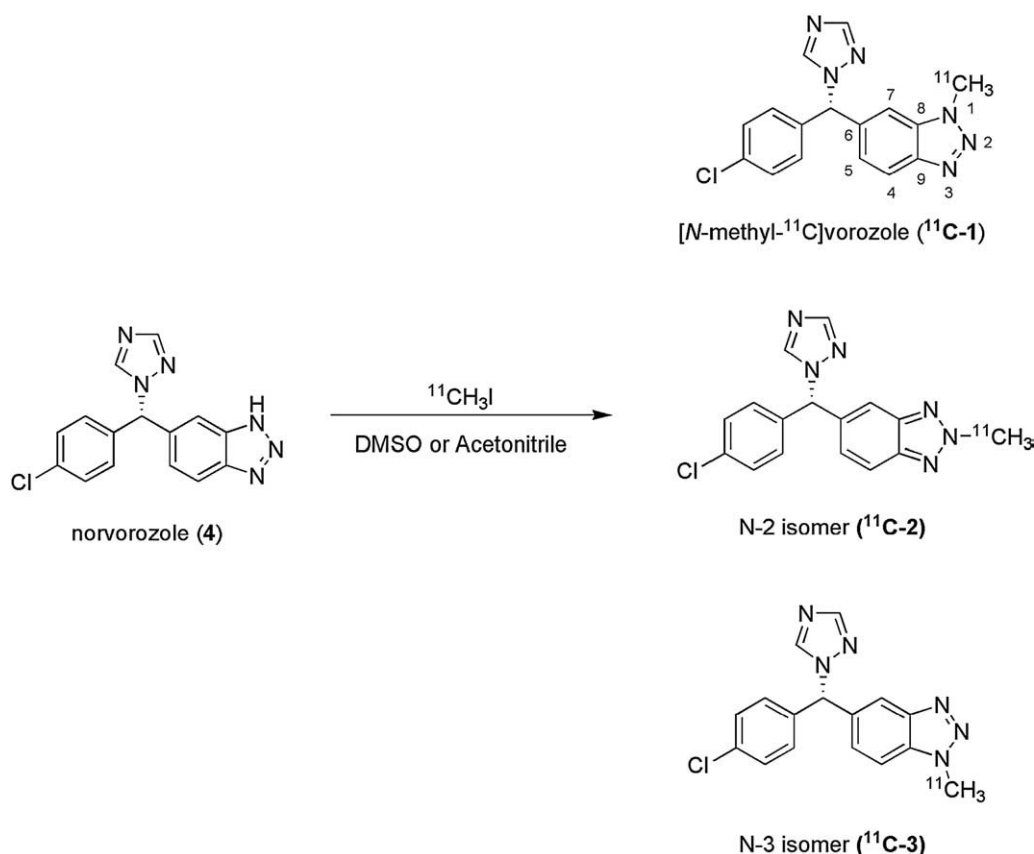
Scheme 1. The radiosynthesis of [N-methyl-^{11}C]vorozole and its isomers.

the first report of the brain distribution and pharmacokinetics and pharmacological blockade of the *pure* [*N*-methyl-^{11}C]vorozole (**[11]C-1**, N-1 isomer) with PET in the female baboon.

2. Materials and methods

2.1. Chemistry

Vorozole and norvorozole and their enantiomers were generously given by Johnson & Johnson Pharmaceutical Research and Development (Beerse, Belgium). All other chemicals and solvents were purchased from Aldrich Chemical (Milwaukee, WI, USA) and were used without further purification. NMR spectra were recorded using a Bruker Avance 400 MHz NMR spectrometer (Bruker Instruments, Billerica, MA, USA). Gas chromatography-mass spectroscopy (GC-MS) analyses were performed with Agilent 6890/5973N GC/MSD system (Agilent Technologies, Avondale, PA, USA) equipped with a DB-5 column (30 m length×0.250 mm inner diameter (ID), 0.25 μm film thickness; injector temperature; split; injection temperature, 280°C; oven temperature, 280°C, isothermal; carrier gas, He; flowrate 1 ml/min). The temperatures of source and quadrupole of mass spectrometer were 280°C and 180°C, respectively.

[^{11}C]Methyl iodide was produced by PETtrace MeI Microlab (GE Medical Systems, Milwaukee, WI, USA) from [^{11}C]carbon dioxide, which was generated from a nitrogen/oxygen (1000 ppm) target [$^{14}N(p,\alpha)^{11}C$] using EBCO TR 19 cyclotron (Advanced Cyclotron Systems, Richmond, Canada). High-performance liquid chromatography (HPLC) purification was performed by a Knauer HPLC system (Sonntek, Woodcliff Lake, NJ, USA) with a model K-5000 pump, a Rheodyne 7125 injector, a model 87 variable wavelength monitor and NaI radioactivity detector.

During the radiosynthesis, ^{11}C was measured by three p-type/intrinsic/n-type (PIN) diode detectors (3×3 mm Si diode, Carroll Ramsey Associates, Berkeley, CA) equipped with a triple-channel amplifier (model 101-HDC-3; Carroll Ramsey Associates, Berkeley, CA, USA) and NI USB-6008 (National Instruments, Austin, TX, USA). Radioactivity of [*N*-methyl-^{11}C]vorozole was measured by a Capintec CRC-712MV radioisotope calibrator (Capintec, Ramsey, NJ, USA). [11]C Radioactivity of preparative HPLC sample was measured by a Packard MINAXI γ 5000 automated gamma counter (Packard Instrument, Meriden, CT, USA). All radioactivity measurements were decay corrected. Specific activity was measured by radioactivity/mass (Ci/μmol). For quality control, radiochemical purities were measured by analytical HPLC using aqueous formic acid solution [0.1% (v/v), pH=2.8]:methanol (1:2) at a flow rate 1 ml/min on a Luna PFP(2) (250×4.6 mm, 5 μm; Phenomenex, Torrance, CA, USA). For baboon studies, a formulation of [*N*-methyl-^{11}C]vorozole in 4 ml of saline was used.

2.1.1. Analysis of reaction products from the reaction of norvorozole with unlabeled methyl iodide

To a solution of (*S*)-norvorozole [6-[(*S*)-(4-chlorophenyl)-1*H*-1,2,4-triazol-1-ylmethyl]-1*H*-Benzotriazole (**4**), 1.3 mg, 4 μmol] in anhydrous acetonitrile (1 ml) was added potassium carbonate (60 mg, 434 μmol) and methyl iodide (180 mg, 0.8 mmol). The reaction mixture was stirred at room temperature for 7 min. After evaporation of acetonitrile and excess of methyl iodide under reduced pressure, the crude product was extracted with ethyl acetate and dried with anhydrous sodium sulfate, filtered then evaporated to dryness using the rotary evaporator under reduce pressure. This crude mixture was separated by HPLC using aqueous formic acid solution (pH=3.0):methanol (45:55) at a flow rate 1 ml/min on a Luna PFP(2) (250×4.6 mm, 5 μm; Phenomenex). The three major fractions of ultraviolet (UV) active peaks (**3**, T_R=21 min; **1**, T_R=24 min; **2**, T_R=35 min) were collected separately (ratio, 1:1:1), and evaporated under reduced pressure. The residual water was extracted with ethyl acetate, dried with anhydrous sodium sulfate, filtered and evaporated to give three analytical samples.

6-[(*S*)-(4-chlorophenyl)-1*H*-1,2,4-triazol-1-ylmethyl]-1-methyl-1*H*-benzotriazole [(*S*)-vorozole, **1**], ^{1}H-NMR (CDCl₃) δ 8.08 (s, 1 H), 8.07 (s, 1 H), 8.06 (d, *J*=9.2, 1 H), 7.39 (d, *J*=8.8 H), 7.19-7.21 (m, 2 H), 7.14 (d, *J*=8.8, 2 H), 6.93 (s, 1 H), 4.26 (s, 3 H). ^{13}C-NMR (CDCl₃) 152.83, 145.99, 143.82, 137.64, 136.01, 135.42, 133.86, 129.89. 129.64, 124.26, 121.04, 108.91, 67.18. 34.61.

5-[(*S*)-(4-chlorophenyl)-1*H*-1,2,4-triazol-1-ylmethyl]-1-methyl-1*H*-benzotriazole (**3**) ^{1}H-NMR (CDCl₃) δ 8.07 (s, 1 H), 8.01 (s, 1 H), 7.79 (s, 1 H), 7.68 (d, *J*=8.8, 1 H), 7.36-7.40 (m, 3 H), 7.11 (d, *J*=8.4, 1 H), 6.91 (s, 1 H), 4.33 (s, 3 H). ^{13}C-NMR (CDCl₃) δ 152.51, 146.24, 143.67, 136.29, 135.23, 133.87, 133.68, 129.60, 129.57, 127.76, 120.17, 110.33, 67.18, 34.66.

5-[(*S*)-(4-chlorophenyl)-1H-1,2,4-triazol-1-ylmethyl]-2-methyl-2H-benzotriazole (**2**) ^{1}H-NMR (CDCl₃) δ 8.06 (s, 1 H), 8.00 (s, 1 H), 7.87 (d, *J*=8.8 Hz, 1 H), 7.53 (s, 1 H), 7.38 (d, *J*=8.5, 2 H), 7.21 (d, *J*=8.9, 1 H), 7.12 (d, *J*=8,5, 2 H), 6.87 (s, 1 H), 4.52 (s, 3 H). ^{13}C-NMR (CDCl₃) δ 152.80, 144.64, 144.51, 143.78, 136.26, 136.12, 135.17, 129.73, 129.53, 126.62, 119.19, 117.96, 67.40, 43.64.

2.1.2. Reaction of nor-vorozole with [^{11}C]methyl iodide

To (*S*)-norvorozole (**4**, 1 mg, 3.22 μmol) in dimethyl-sulfoxide (300 μl) was added 5 M KOH (1 μl, 1.6 eq). After vortexing for 30 sec, the reaction mixture was transferred into a 1.5-ml V-shape reaction vessel. [^{11}C]methyl iodide was transferred in a helium stream from the GE Medical Systems methyl iodide system into this solution at room temperature, and peak trapping was observed by a pin-diode detector. After the vessel was heated to 90°C for 3 min, the reaction mixture was cooled and diluted with HPLC eluent (1 ml). Preparative HPLC was performed using a method simulating the original publication method for the synthesis of [*N*-methyl-^{11}C]

vorozole (Method A) and another which we developed to separate [N-methyl-^{11}C]vorozole from [11]C-2 and [11]C-3 (Method B).

2.1.2.1. Method A (partial separation).

We slightly modified the original HPLC method [17] based on column availability. Briefly, the reaction residue diluted with HPLC solvent (1 ml) was subjected to HPLC chromatography on a Spherisorb ODS2 (Phenomenex, 250×10 mm, 5 μm) column using aqueous ammonium formate solution (50 mM, pH=3.5):acetonitrile (65:35), and a flow rate of 5 ml/min. The major ^{11}C-labeled fraction (fraction **X**) was collected at the expected retention time (T_R=15 min) for vorozole and the other minor radioactive fraction was collected at 22 min. The 15 and 22-min fractions were present in a ratio of 2:1, respectively. The solvent was removed from the 15-min fraction, and it was rechromatographed on a pentafluor-ophenylpropyl (PFPP) based column (Luna PFP(2), Phe-nomenex, 250×0.46 mm, 5 μm) column with aqueous formic acid (0.1%(v/v, pH=2.8):methanol (1:2) and flow rate of 1 ml/min to reveal two peaks of equal radioactivity at 10 and 11 min.

2.1.2.2. Method B (complete separation).

The crude product in DMSO was diluted with of HPLC solvent (1 ml) and chromatographed using a solvent mixture of aqueous formic acid solution (0.1% (v/v), pH=2.8): methanol (45:55) at a flow rate 5 ml/min on a Luna PFP (2) (Phenomenex, 250 mm×10 mm, 5 μm). [N-methyl-^{11}C] vorozole ([11]C-1) eluted at 24.5 min and was collected. The HPLC solvent was removed by azeotropic evaporation with acetonitrile using a rotary evaporator under the reduced pressure. The residue was taken up by saline (4 ml), filtered through a 0.2 μm HT tuffryn membrane filter (Acrodisc 25 mm Syringe Filter, Pall Life Sciences, Ann Arbor, MI) into a sterile vial ready for the baboon study. The radiochemical purity for [11]C-1 was >99% as determined by TLC (solvent, acetonitrile:water:NH$_4$OH (conc.)=90:9:1) on Macherey-Nagel plastic back silica plates (R_f: 0.6). In separate syntheses, fractions containing [11]C-2 and [11]C-3 (which eluted at 21.2 and 39.5 min respectively) were collected.

2.2. Measurement of log D

Log $D_{7.4}$ for ^{11}C-1, [11]C-2 and [11]C-3 was measured using a published method [23,24]. Briefly, into a mixture of 1-octanol (2.5 ml) and phosphate buffered saline (pH 7.4; 2.5 ml) was added an aliquot (50 μl) of ^{11}C solution. The mixture was vortexed for 2 min and then centrifuged at 7000 rpm for 2 min. An aliquot (0.1 ml) of the clear octanol layer and 1.0 ml of the buffer layer were sampled separately into two empty vials and counted; 2 ml of the octanol layer was transferred into a test tube containing 0.5 ml of fresh octanol and 2.5 ml of buffer. After vortexing and centrifuging in the same way as the first measurement, counts of the second

batch were measured. In general, these processes were repeated up to six times. Log $D_{7.4}$ at pH=7.4 is as the $\log_{10}$ of the average of the ratios of the decay corrected counts in the octanol: phosphate buffer (pH=7.4).

2.3. Measurement of free fraction in plasma

An aliquot of ^{11}C-1, [11]C-2 or [11]C-3 was incubated at room temperature for 10 min with baboon plasma (500 μl) as described previously [24]. Briefly, aliquots (20-40 μl) of the incubated spike plasma were counted (unspun aliquots). A portion of the incubation mixture (200–400 μl) was centrifuged using a Centrifree tube (Amicon, Beverly, MA, USA; molecular weight cutoff, 30,000) for 10 min. The top portion of the Centrifree tube (the bound portion) was removed and precisely measured aliquots (20–40 μl) of the liquid in the cup (unbound fraction) were counted. The free fraction is the ratio of radioactivity of the unbound aliquots to the radioactivity of the unspun aliquots. All counts were decay-corrected.

2.4. PET studies in baboons

All animal studies were reviewed and approved by the Brookhaven Institutional Animal Use and Care committee. Four different baboons were studied in seven PET sessions where two or three radiotracers injections were administered two hours apart to compare different isomers or to assess reproducibility of repeated measures or the effects of a blocking dose of vorozole or letrozole (0.1 mg/kg, 5 min prior). Baboons were anesthetized with ketamine (10 mg/kg) and then intubated and ventilated with a mixture of isoflurane (Forane, 1–4%) and nitrous oxide (1500 ml/min) and oxygen (800 ml/min). Animals were transported to and from the PET facility in a temperature controlled transfer cage and a member of the staff attended them while they recovered from anesthesia. Catheters were inserted in a popliteal artery and radial arm vein for arterial sampling a radiotracer injection respectively. Dynamic PET imaging was carried out on a Siemen's HR+high resolution, whole body PET scanner (4.5×4.5×4.8 mm at center of field of view) in 3D acquisition mode, 63 planes. A transmission scan was obtained with a [68]Ge rotating rod source before the emission scan to correct for attenuation before each radiotracer injection. The injected dose of ^{11}C-1, [11]C-2 or [11]C-3 ranged from 55.5 to 185 MBq; the specific activity ranged from 16 to 19 Ci/μmol at the end of the bombardment, and the injected mass ranged from 0.08–0.3 nmol. Dynamic scanning was carried out for 90 min with the following time frames (1×10 s, 12×5 s, 1×20 s, 1×30 s, 8×60 s, 4×300 s and 8×450 s). Arterial sampling was performed to obtain the time activity curve in plasma and to analyze selected samples for the fraction of ^{11}C present as unchanged parent compounds with the sample times described previously [24]. During the PET scan, baboons were monitored for heart rate, respiration rate, PO$_2$ and temperature. Animals were allowed 4 weeks between studies to recover from anesthesia and blood sampling.

2.4.1. Plasma analysis for fraction of ^{11}C-1, [11]C-2 and [11]C-3

Plasma samples at 1, 5, 10, 30 and 60 min were analyzed by HPLC to determine the percent of residual parent tracer. Plasma samples from selected time points were added to 300 μl acetonitrile containing an appropriate amount of standard, then subjected to cell disruption using a Polytron (Brinkmann Instruments), centrifuged for 4 min and decanted into 300 μl water. HPLC conditions were 60:40 0.1 M ammonium formate:acetontrile, Waters μBondapak column (3.9×300 mm), flow 1.3 ml/min and UV detection at 254 nm. Supernatants were injected onto the column, reserving a measured amount to determine recovery of injected activity from the column. Retention times were 7.5 min for vorozole itself and the N-3 isomer and 9.5 min for the N-2 isomer. Five fractions were collected from each injection, three before the parent peak, the parent peak and, finally, the tail of the parent peak. The percent unchanged tracer was determined by dividing the sum of the last two peaks by the sum of all HPLC fractions. Sample recoveries were determined to verify that there were no labeled metabolites retained on the column.

2.4.2. Image analysis

Time frames were summed over the 90-min experimental period. Regions of interest were placed over the amygdala, the preoptic area, frontal cortex, cerebellum and thalamus on the summed image and then projected onto the dynamic images to obtain time activity curves. Regions occurring bilaterally were averaged. [11]C concentration in each region of interest was divided by the injected dose to obtain the % dose/cc. The summed PET images from one baboon was coregistered with a 3D magnetic resonance image of the same animal using PMOD (PMOD Technologies).

3. Results and discussion

3.1. Reaction of norvorozole (4) with [^{12}C]methyl iodide

[N-methyl-^{11}C]Vorozole synthesized by the published method [17] using slightly modified HPLC purification conditions, did not give the high signal-to-noise baboon
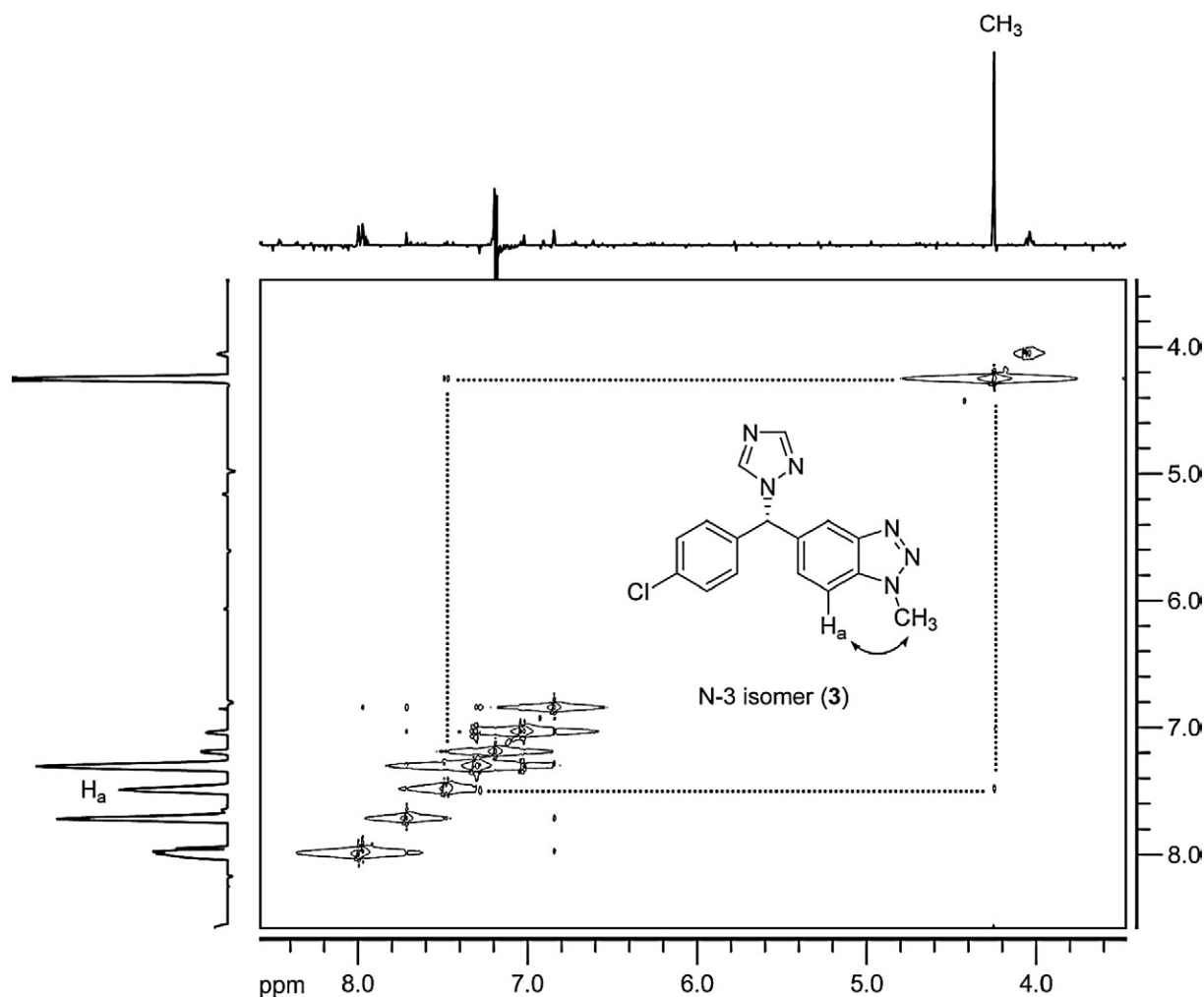

Fig. 1. The 2D-NOESY spectrum of N-3 isomer (3) acquired in CDCl₃ at 400 MHz.

brain images and autoradiography results with rat brain sections which were described previously (data not shown). Given the alkaline reaction medium, we first considered that the nonspecific binding could be a result of racemization, thus forming the inactive (R)-vorozole [25], which would coelute with the active form. However, chiral HPLC analysis (column, Chiralpak OJ-P, 4.6×15 mm; eluent, water: acetonitrile=75:35; flowrate, 0.5 ml/min) indicated that no racemization of either (S)-norvorozole or (S)-vorozole occurred under the reaction conditions (data not shown).

Serendipitously, during this investigation, we uncovered the presence of an unexpected reaction byproduct (therefore observing three N-methylated compounds in total) that was formed in approximately equal yield to (S)-vorozole. This product was not separable under the HPLC conditions originally reported, and thus, Lidström et al. [17] noted only two major fractions "in a ratio of 5 to 2." The authors identified the two fractions as {[N-methyl-^{11}C]vorozole (N-1 alkylation)} and an regioisomer, **[11]C-3** (N-3 alkylation). Their assignment was based on ^{13}C NMR experiments, in which [^{13}C]methyl iodide was added as a carrier in the ^{11}C methylation reaction in order to have sufficient mass for a ^{13}C NMR. After HPLC isolation of the fraction with the expected retention time of vorozole, the authors determined the chemical shift of the ^{13}C-enriched product matched that of vorozole (34.4 ppm). The minor isomer, which was well separated under their HPLC conditions, was also isolated and analyzed by ^{13}C NMR and assigned as the N-3

methylation product with a reported chemical shift of 43.4 ppm [17]. When we reproduced the original radiosynthesis as closely as possible [Spherisorb octadecyl-bonded silica (ODS) columns (Phenomenex) were used instead of Spherisorb ODS1 (Beckman) because of commercial availability] [17], we also found two apparent ^{11}C labeled fractions in a similar ratio (2:1).

Since there was precedent for alkylation at the N-2 position of benzotriazole rings [26], we investigated the possibility that the N-2 isomer may form and that it may coelute with the labeled vorozole accounting for the low specificity and reproducibility we had observed in our PET studies. In fact, GC-MS analysis confirmed that three products were formed by the reaction of norvorozole with excess methyl iodide. Consistent with our hypothesis, each of the three isomers had the same molecular weight (M^+=324) yet fragmented distinctly. Later, we observed three singlet peaks between 4.2–4.6 ppm in the ^{1}H-NMR spectrum. The ^{13}C-NMR spectrum of the crude reaction mixture also confirmed three methyl peaks, 34.61, 34.66 and 43.64 ppm. However, in spite of rigorous HPLC analysis with six different reversed-phase and two different normal-phase columns using several gradient elution systems, only two major fractions were observed. This prompted us to isolate and characterize the two major UV-active fractions from HPLC separation in order to confirm that the vorozole fraction was contaminated by one of the other isomers. GC-MS and ^{13}C-NMR analysis of the fraction assigned as
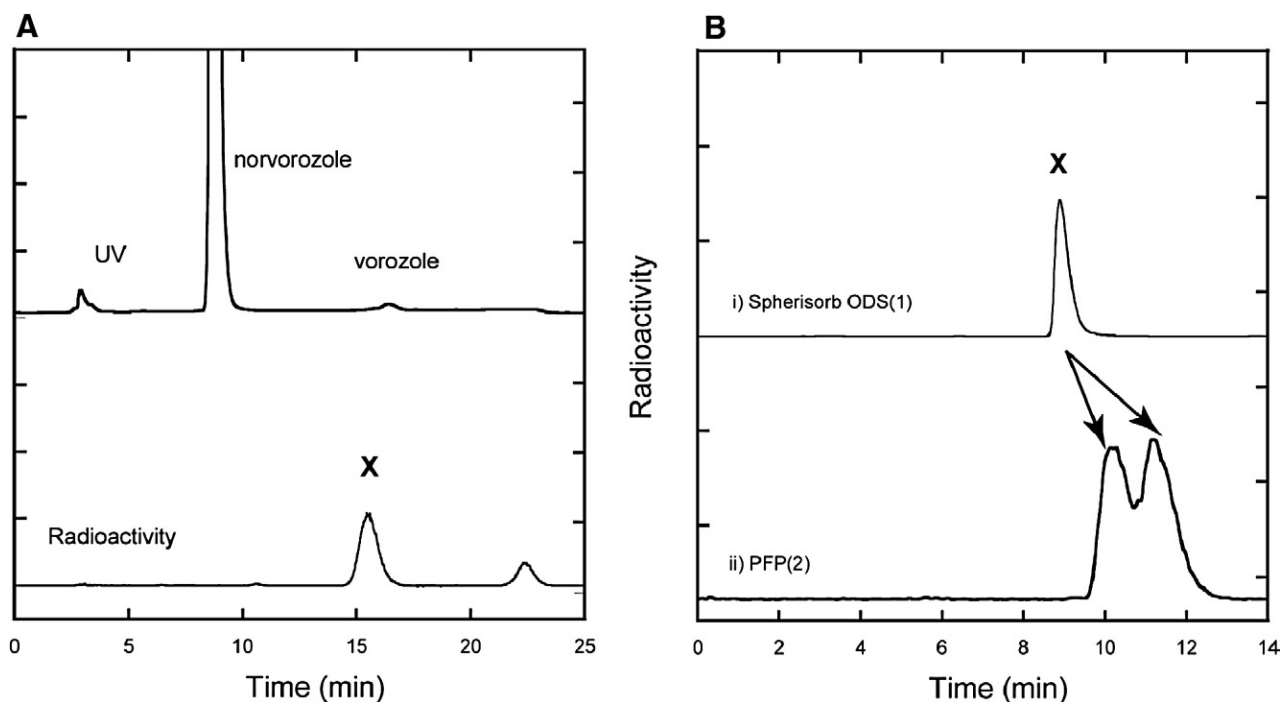

Fig. 2. (A) Preparative HPLC profile of the crude reaction mixture from the alkylation of norvorozole with [^{11}C]methyl iodide. HPLC conditions: Spherisorb ODS (2), Phenomenex, 5 mm, 250×10 mm; eluent, ammonium formate buffer (50 mM, pH=3.5)/acetonitrile (65/35), 5 ml/min. Fraction **X** was isolated and subjected to analytical HPLC. (B) Comparison of HPLC analysis of the isolated vorozole fraction, **X** in the reported system (i) and new HPLC system (ii). (i) Spherisorb ODS (1), Phenomenex, 5 μm, 250×4.60 mm; eluent, ammonium formate buffer (50 mM, pH=3.5)/acetonitrile (40/60), 1 ml/min. (ii) Luna PFP (2), Phenomenex, 5 μm, 250×4.6 mm; eluent, aqueous formic acid adjusted to pH=3.0/methanol (1/2), 1 ml/min.
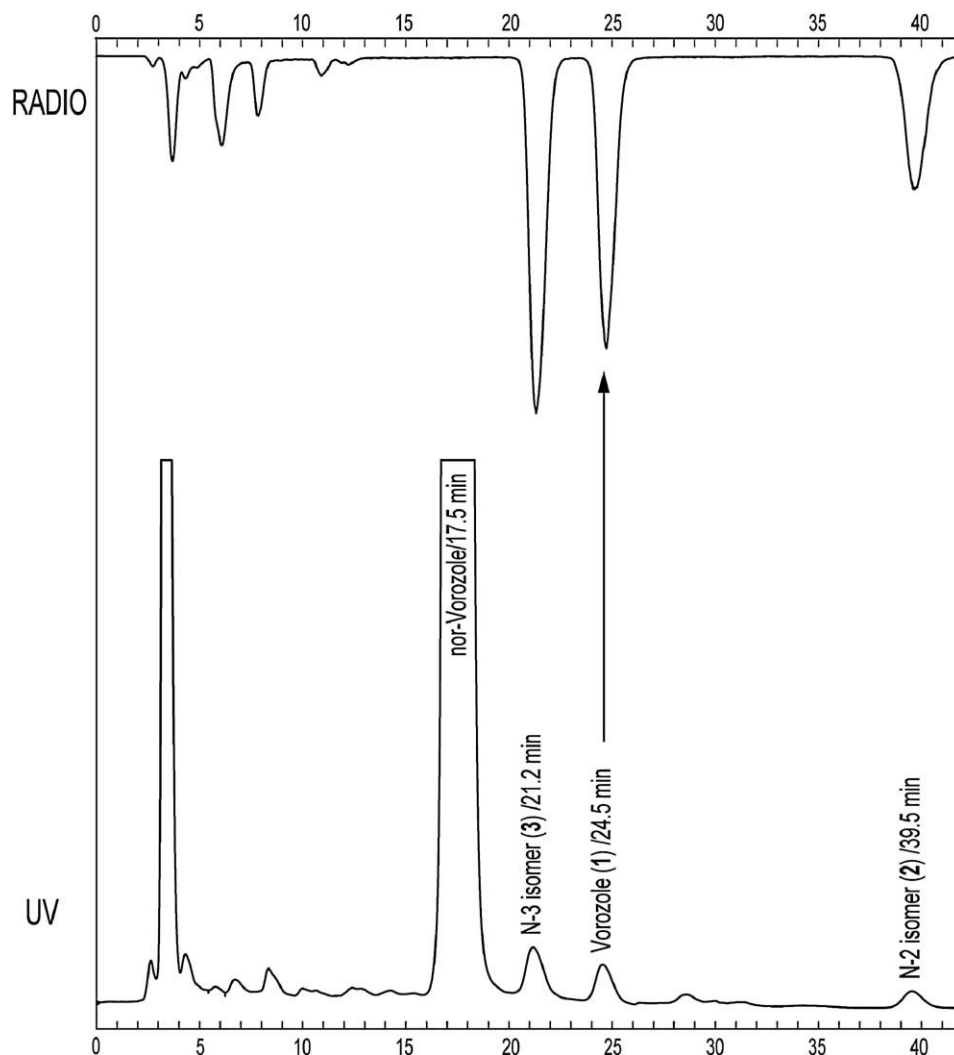
Fig. 3. Preparative HPLC profile of the crude reaction mixture from the alkylation of norvorozole with [11C]methyl iodide. Baseline separation of [N-methyl-11C] vorozole from 11C-2 and 11C-3 was achieved. HPLC conditions: Luna PFP(2) (Phenomenex, 250 mm×10 mm, 5 μm); aqueous formic acid adjusted to pH=3)/ methanol (45/55); 5 ml/min.

vorozole confirmed the presence of two isomers of the same molecular weight with 13C-methyl shifts of 34.61 and 34.66 ppm (125 MHz, CDCl3), one of which (34.61 ppm) corresponded to the chemical shift of an authentic sample of vorozole. These two shifts are so similar that they were probably not resolved at the lower field strength used in the original analysis. Thus, this rigor of analysis, which has been typical in the field of 11C labeling radiosynthesis was, in this instance, unable to distinguish the two isomers and thus led to PET evaluation of a mixture.

To achieve this exceptionally difficult separation of the three isomers for full characterization, we screened a number of methods for purification. Separation of the two co-eluting isomers in the ODS column was finally achieved (T_R=52 and 58 min) using aqueous formic acid (pH=3.5)/methanol (50:50) at a flowrate (1 ml/min) on a silica based phenoxypropyl bonded column (Synergi PolarRP, 5 μm, 250×4.6 mm, Phenomenex). After isolation, each compound

was characterized by 13C-NMR and 2D-NOESY NMR. The byproduct that could be isolated in pure form using the original ODS HPLC conditions (13C of N-methyl, 43.64 ppm), which was previously assigned as the N-3 methylated isomer (3), was re-assigned as the N-2 isomer (2). This reassignment was primarily based on the 13C chemical shift of the two quaternary carbons (both C-8 and C-9, above 140 ppm) of the benzoquinoid ring, which were shifted clearly downfield relative to the corresponding one of benzotriazole carbons which is typically below 140 ppm [27]. The other

Table 1
Comparison of log D and free fraction in plasma for 11C-1, [N-methyl-11C] vorozole, 11C-2 and 11C-3

Isomer log D at pH 7.4 (n=4), percent unbound in plasma (n=2)		
11C-1	2.5	7.2
11C-2	2.9	4.6
11C-3	2.5	8.1

two isomers, which co-eluted under the original HPLC conditions but which were separated by the PFPP column, were identified as vorozole (N-1 isomer) and the N-3 isomer (**3**). Their structural assignments were largely based on the nuclear Overhauser effect correlation of the H-7 or H-4 to the methyl group (Fig. 1).

3.2. Alkylation of norvorozole with [¹¹C]methyl iodide: reproduction of the previous synthesis [17,18] and separation of [N-methyl-¹¹C]vorozole from ¹¹**C-3** and ¹¹**C-2**

Initially, we set out (1) to reproduce the previous radiosynthesis and HPLC conditions (observation of two radioactive fractions) and (2) to separate the "vorozole" fraction if it was actually a mixture of vorozole and the N-3 isomer as our ¹²C synthesis results suggested. Since the HPLC column (Spherisorb ODS1, Beckman, 250×10 mm) used previously was not commercially available, we replaced it with a similar HPLC column [Spherisorb ODS (2), Phenomenex, 5 μm, 250×10 mm). Similar to the previous report, we obtained only two radioactive fractions in a ratio of 2:1. The major radioactive 15-min fraction **X** (Fig. 2A), which has the same retention time as vorozole, was isolated and subjected to further analysis (Fig. 2B) using an analytical HPLC system. We chose the same solvent system and a similar HPLC column [Spherisorb ODS (1), Phenomenex, 5 μm, 250×4.60 mm) to that reported previously [17,18]. The radioactive fraction, **X**, showed only one peak in this system (Fig. 2B). Other conventional ODS columns gave the same results using various solvent

systems (data not shown). However, a PFPP bonded-phase HPLC column resolved the 15-min fraction **X** into two peaks, which have the same retention time as "cold" N-3 isomer (**3**) and vorozole (**1**), respectively (Fig. 2B). Later, all three regioisomers of the crude reaction mixture were well separated using a semipreparative scale PFPP column (Fig. 3). The radiochemical yields of the three regioisomers were approximately 30% each. The radiochemical purity was >97%, and the specific activity ranged 10–19 Ci/μmol (0.3–0.7 GBq/μmol). The total radiosynthesis time was 65 min after the end of the cyclotron bombardment.

3.3. Comparison of ¹¹C labeled fraction A (¹¹C-1+¹¹C-3), [N-methyl-¹¹C]vorozole (¹¹**C-1**), ¹¹**C-3** and ¹¹**C-2** in the baboon brain

We determined that all three regioisomers have a lipophilicity (log $D_{7.4}$) considered suitable for blood–brain barrier penetration. Notably, the log D's of ¹¹**C-1** and ¹¹**C-3** were almost identical (Table 1), which is consistent with their coelution on HPLC using the ODS column. The free fraction of ¹¹**C-1** and ¹¹**C-3** in baboon plasma was also similar.

Fig. 4 compares PET images of the 15-min fraction (mixture of ¹¹**C-1** and ¹¹**C-3**), ¹¹**C-1**, ¹¹**C-3** and ¹¹**C-2** at the levels of the amygdala (top row) and preoptic area (bottom row). These images showed (1) low signal to background of the aromatase-rich amygdala and no specific uptake in the POA for the mixture, (2) high retention in amygdala and preoptic area for [N-methyl-¹¹C]vorozole and (3) no specific uptake in amygdala and preoptic area for ¹¹**C-3** and ¹¹**C-2**. Low signal to background for the mixture is consistent with
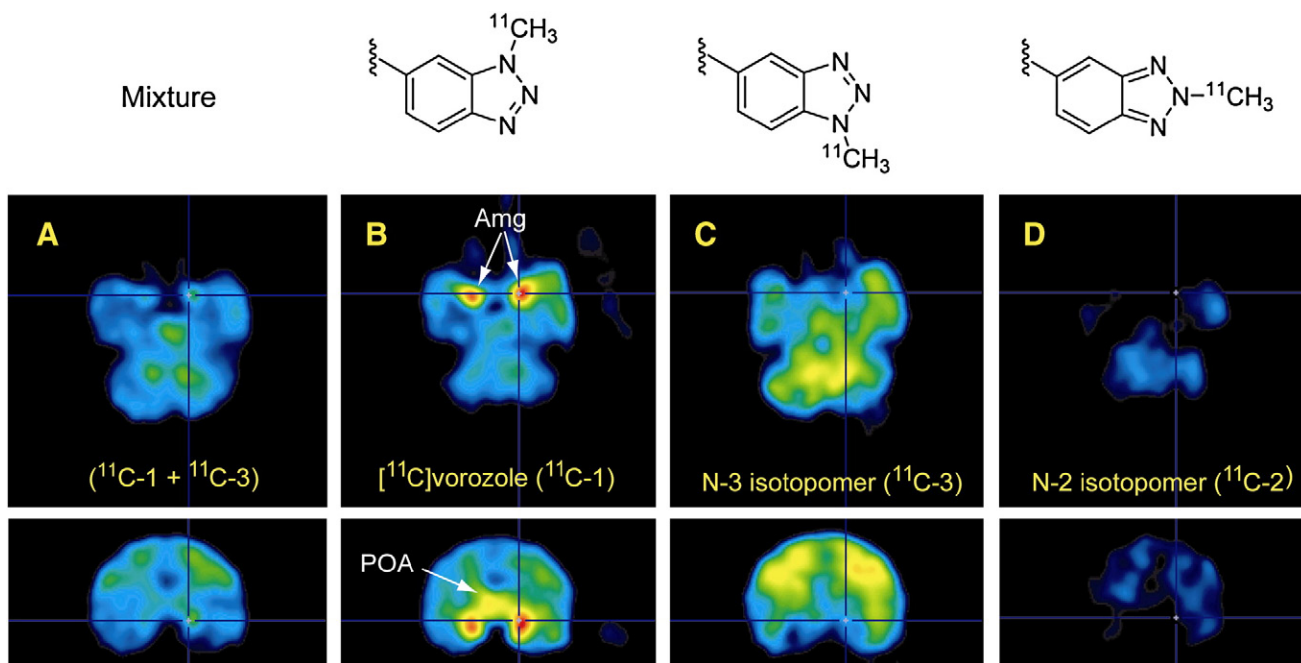

Fig. 4. PET images in the (transaxial (top row) and coronal (bottom row) planes in baboon brain summed from 15–90 min after injection for (A) the 15-min fraction (**X**), [¹¹**C-1**+¹¹**C-3**, 176.49 MBq (4.77 mCi)], (B) [N-methyl-¹¹C]vorozole [¹¹**C-1**, 163.91 MBq (4.43 mCi)]; (C) N-3 isomer [¹¹**C-3**, 123.21 MBq (3.33 mCi)] and (D) N-2 isomer [¹¹**C-2**, 44.77 MBq (1.21 mCi)]. All PET images are dose-corrected. Arrows indicate the amygdala (Amg) and POA.

contamination with the N-3 isomer (^{11}C-3). The high signal to noise in the amygdala and preoptic areas for pure ^{11}C-1 was consistent with the high affinity of vorozole for aromatase. We note that affinity values for the two nonvorozole isomers (2 and 3) for aromatase are not available, though we would predict low affinities relative to vorozole (IC$_{50}$=2.7 nM) [28] based on our imaging results.

Time-activity curves for pure [*N*-methyl-^{11}C]vorozole (^{11}C-1) in the baboon brain revealed very high initial uptake in five brain regions (amygdala, cerebellum, frontal cortex, white matter and preoptic area). ^{11}C peaked at ~5 min and cleared to a low point at 20–30 min and relatively stable accumulation through the end of the study in all brain regions (Fig. 5A). Regions with the highest accumulation of radiotracer were the amygdala and the preoptic area, both of

which are rich in aromatase. Pretreatment with "cold" vorozole or letrozole (data not shown for letrozole) reduced [*N*-methyl-^{11}C]vorozole (^{11}C-1) accumulation in all brain regions examined, indicating its specificity to brain aromatase. This is shown in Fig. 5B, which compares the baseline and the blocked time-activity curves for the amygdala and the preoptic areas only. Note that, after vorozole treatment, there is a rapid but lower initial uptake followed by a steady clearance and *no accumulation* for both brain regions. A similar pattern after pretreatment was seen for other brain regions (data not shown). This can be also clearly seen from the images with the coregistered and blocking views (Fig. 6). Kinetic modeling is currently underway.

Both ^{11}C-3 and ^{11}C-2 (which we report here for the first time) show reasonably high brain penetration (0.02–0.03%

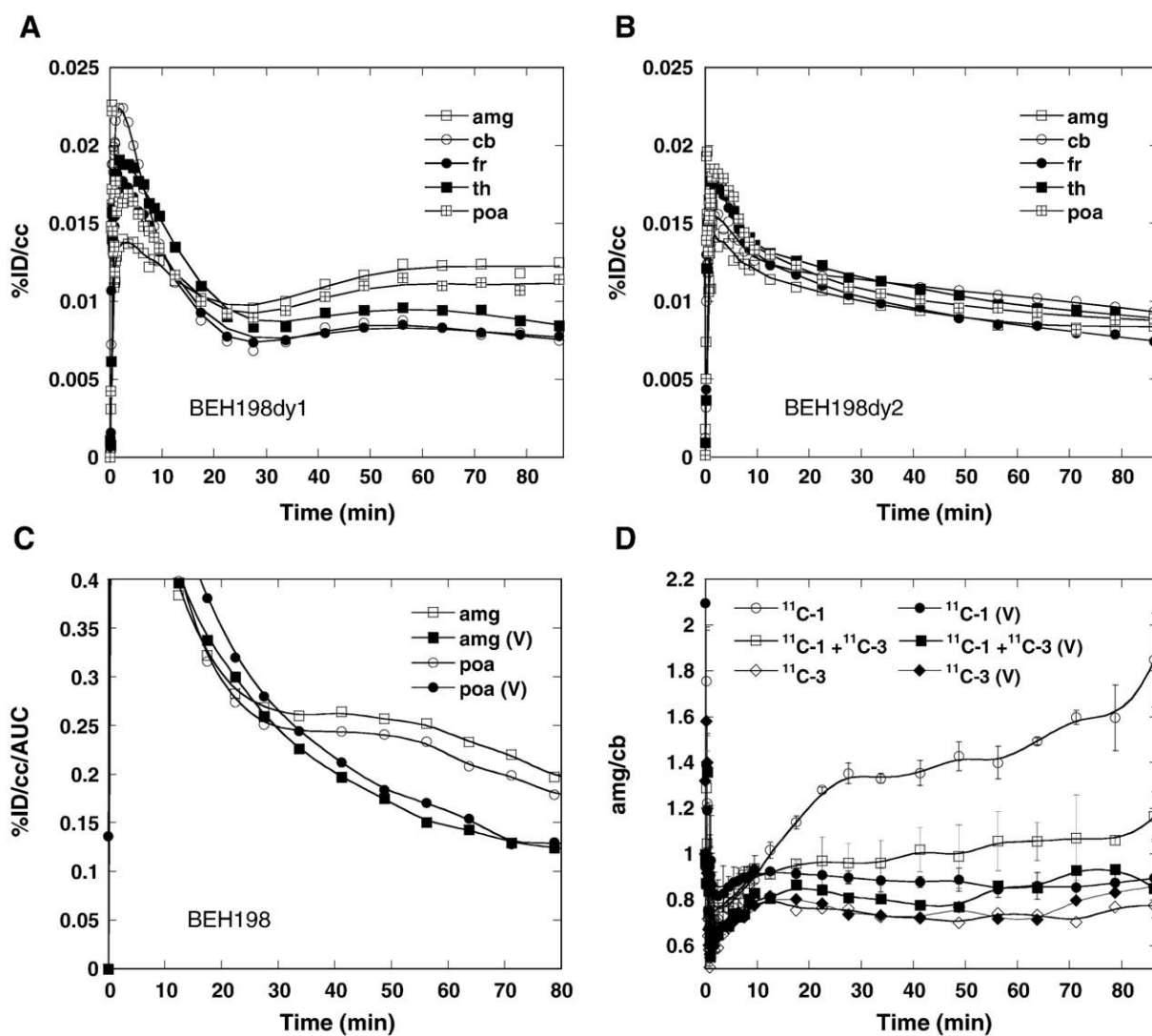

Fig. 5. Comparison of time–activity curves for [*N*-methyl-^{11}C]vorozole in the baboon brain over a 90 minute scanning session at baseline [^{11}C-1, 163.91 MBq (4.43 mCi)] (A), after treatment with vorozole (0.1 mg/kg, 5 min prior) [^{11}C-1, 173.16 MBq (4.68 mCi)] (B), time-activity curves for amygdala and preoptic areas corrected for the area under the plasma time-activity curves (AUC) at baseline(open symbols) and after pretreatment with vorozole (closed symbols) (C). (D) Ratio of amygdala/cerebellum vs time for ^{11}C-1 (*n*=3), mixture (^{11}C-1+^{11}C-3, *n*=2), and N-3 isomer (^{11}C-3, n=1) at baseline and after pretreatment with vorozole in baboons. amg, amygdala; cb, cerebellum; fr, frontal cortex; th, thalamus; poa, preoptic area; V, vorozole.
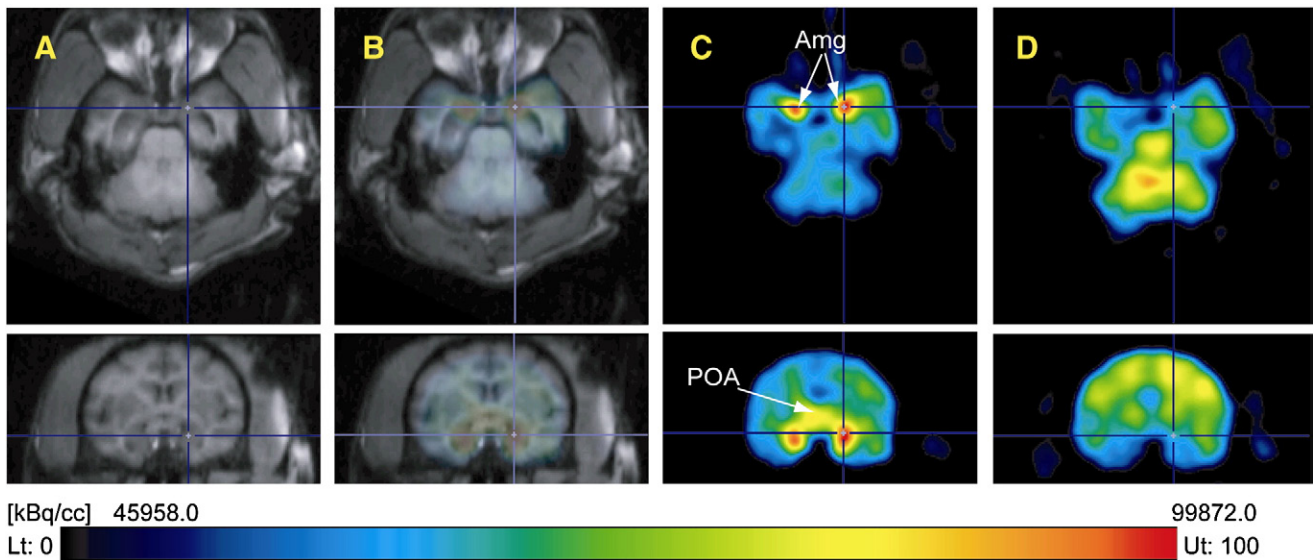
Fig. 6. Comparisons of [*N*-methyl-^{11}C]vorozole ([11]**C-1**) PET images in the same baboon brain in transaxial (top row) and coronal (bottom row) view between baseline and pretreatment with vorozole (**1**). (A) MR images. (B) coregistered [11]**C-1** PET and MR images. (C), [*N*-methyl-^{11}C]vorozole [[11]**C-1**, 163.91 MBq (4.43 mCi)] PET images. (D) PET images following pretreatment with vorozole (0.1 mg/kg) 5 min before the injection of [methyl-^{11}C]vorozole [[11]**C-1**, 173.16 MBq (4.68 mCi)]. All PET images were summed over 15-90 min and PET image (D) was dose-corrected based on (C).

ID/cc at 2.5 min, data not shown), but no specific distribution to aromatase-rich brain regions as was shown in the images in Fig. 4.

3.4. Analysis of chemical form of ^{11}C in plasma after administration of ^{11}C-1, [11]C-2 and [11]C-3 in the baboon

For all baboon studies, total ^{11}C in plasma was measured and the unchanged fraction of ^{11}C-labeled compound was determined by HPLC. The % unchanged ^{11}C labeled vorozole ([11]**C-1**) in baboon plasma was high (up to 78–

80% at 90 min). Interestingly, the position of the methyl group seems to exert a considerable effect on the metabolism, in that N-2 and N-3 isomers showed very rapid appearance of labeled metabolites and intersubject variability seemed high compared with N-1([11]**C-1**). However, the area under curves (AUCs) for [11]**C-1**, [11]**C-3** in plasma normalized to the injected dose over 90 min were similar as shown Fig. 7B, suggesting that the contribution of the N-3 isomer in the PET image of the mixture ([11]**C-1**+[11]**C-3**) would be significant. The N-2 isomer ([11]**C-2)**
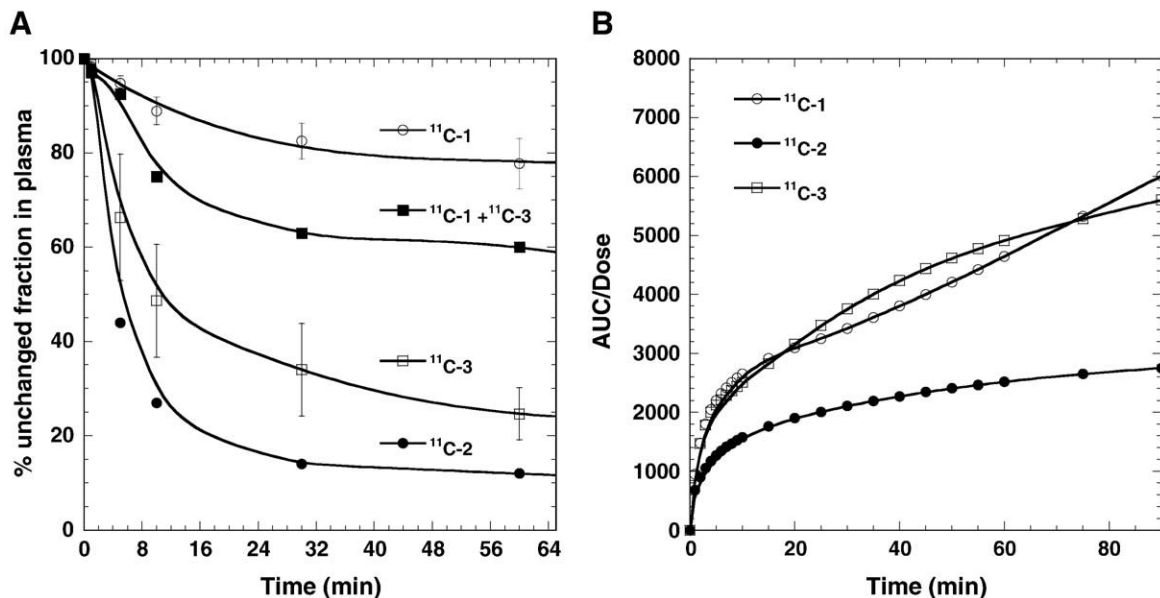
Fig. 7. (A) The percentage of unchanged ^{11}C labeled fraction **X** ([11]**C-1**+[11]**C-3**), vorozole ([11]**C-1**), N-2 isomer ([11]**C-2**), and N-3 isomer ([11]**C-3**) in baboons. (B) The time-AUC plots of ^{11}C-labeled vorozole ([11]**C-1**), N-2 isomer ([11]**C-2**) and N-3 isomer ([11]**C-3**) in baboons.

showed a rapid rate of disappearance of the parent labeled compound from plasma.

4. Conclusion

We reinvestigated the synthesis of [*N*-methyl-^{11}C]vorozole and discovered that all three isomers are produced. We characterized each of the isomers by ^{13}C-NMR and by 2D-NOESY spectra and developed a rapid HPLC system to separate [*N*-methyl-^{11}C]vorozole from the N-3 isomer using a pentafluorophenylpropyl bonded silica HPLC column. PET studies of the pure [*N*-methyl-^{11}C]vorozole revealed accumulation of ^{11}C in all brain regions with highest accumulation in the aromatase rich amygdala and POA. Accumulation in these brain regions as well as other brain regions could be blocked by pretreatment with vorozole or letrozole, in accordance with reports indicating that some level of aromatase expression is present in many brain regions. The significant image degradation caused by the contamination of the labeled vorozole with an equal amount of [11]**C-3** brings to light the fact that [*N*-methyl-^{11}C]vorozole will be a significantly better radiotracer than the original data indicated. Our findings necessitate the re-evaluation [*N*-methyl-^{11}C]vorozole data from previous studies, both in vivo and vitro. The availability of pure [*N*-methyl-^{11}C]vorozole for PET represents a new scientific tool for studies of the biology of aromatase and for drug research and development.

Acknowledgment

References

[1] Naftolin F, Ryan KJ, Petro Z. Aromatization of androstenedione by limbic system tissue from human foetuses. J Endocrinol 1971;51: 795–6.

[2] Lephart ED. A review of brain aromatase cytochrome P450. Brain Res Rev 1996;22:1–26.

[3] Garcia-Segura LM, Veiga S, Sierra A, Melcangi RC, Azcoitia I. Aromatase: a neuroprotective enzyme. Prog Neurobiol 2003;71:31–41.

[4] Ishunina TA, van Beurden D, van der Meulen G, Unmehopa UA, Hol EM, Huitinga I, et al. Diminished aromatase immunoreactivity in the hypothalamus, but not in the basal forebrain nuclei in Alzheimer's disease. Neurobiol Aging 2005;26:173–94.

[5] Roselli CF. Brain aromatase: roles in reproduction and neuroprotection. J Steroid Biochem Mol Biol 2007;106:143–50.

[6] Stocco C. Aromatase expression in the ovary: hormonal and molecular regulation. Steroids 2008;73:473–87.

[7] Roselli CE, Resko JA. Cytochrome P450 aromatase (CYP19) in the non-human primate brain: distribution, regulation, and functional significance. J Steroid Biochem Mol Biol 2001;79:247–53.

[8] Yague JG, Wang ACJ, Janssen WGM, Hof PR, Garcia-Segura LM, Azcoitia I, et al. Aromatase distribution in the monkey temporal neocortex and hippocampus. Brain Res 2008;1209:115–27.

[9] Recanatini M, Cavalli A, Valenti P. Nonsteroidal aromatase inhibitors: recent advances. Med Res Rev 2002;22:282–304.

[10] Lonning PE. Pharmacological profiles of exemestane and formestane, steroidal aromatase inhibitors used for treatment of postmenopausal breast cancer. Breast Cancer Res Treat 1998;49:S45–52.

[11] Parkinson AB, Evans NA. Anabolic androgenic steroids: a survey of 500 users. Med Sci Sport Exerc 2006;38:644–51.

[12] Hartgens F, Kuipers H. Effects of androgenic-anabolic steroids in athletes. Sports Med 2004;34:513–54.

[13] Kadi F. Cellular and molecular mechanisms responsible for the action of testosterone on human skeletal muscle. A basis for illegal performance enhancement. Br J Pharmacol 2008;154:522–8.

[14] Wouters W, Decoster R, Krekels M, Vandun J, Beerens D, Haelterman C, et al. R-76713, a new specific non-steroidal aromatase inhibitor. J Steroid Biochem Mol Biol 1989;32:781–8.

[15] Decoster R, Wouters W, Bowden CR, Bossche HV, Bruynseels J, Tuman RW, et al. New nonsteroidal aromatase inhibitors — focus on R76713. J Steroid Biochem Mol Biol 1990;37:335–41.

[16] Decoster R, Vanginckel RF, Callens MJL, Goeminne NKG, Janssens BLE. Antitumoral and endocrine effects of (+)-vorozole in rats bearing dimethylbenzanthracene-induced mammary-tumors. Cancer Res 1992; 52:1240–4.

[17] Lidstrom P, Bonasera TA, Kirilovas D, Lindblom B, Lu L, Bergstrom E, et al. Synthesis, in vivo rhesus monkey biodistribution and in vitro evaluation of a C-11-labelled potent aromatase inhibitor: [*N*-methyl-C-11]vorozole. Nucl Med Biol 1998;25:497–501.

[18] Takahashi K, Bergstrom M, Frandberg P, Vesstrom EL, Watanabe Y, Langstrom B. Imaging of aromatase distribution in rat and rhesus monkey brains with [C-11]vorozole. Nucl Med Biol 2006;33:599–605.

[19] Takahashi K, Tamura Y, Watanabe Y, Langstrom B, Bergstrom M. Alteration in [C-II]vorozole binding to aromatase in neuronal cells of rat brain induced by anabolic androgenic steroids and flutamide. Neuroreport 2008;19:431–5.

[20] Kirilovas D, Bergstrom M, Bonasera TA, Bergstrom-Pettermann E, Naessen T, Holte J, et al. In vitro evaluation of aromatase enzyme in granulosa cells using a [C-11]vorozole binding assay. Steroids 1999; 64:266–72.

[21] Kirilovas D, Naessen T, Bergstrom M, Bergstrom-Petterman E, Carlstrom K, Langstrom B. Characterization of [C-11]vorozole binding in ovarian tissue in rats throughout estrous cycle in association with conversion of androgens to estrogens in vivo and in vitro. Steroids 2003;68:1139–46.

[22] Kirilovas D, Chaika A, Bergstrom M, Bergstrom-Petterman E, Carlstrom K, Nosenk J, et al. Granulosa cell aromatase enzyme activity: Effects of follicular fluid from patients with polycystic ovary syndrome, using aromatase conversion and [C-11]vorozole-binding assays. Gynecol Endocrinol 2006;22:685–91.

[23] Delrosario RB, Jung YW, Baidoo KE, Lever SZ, Wieland DM. Synthesis and in-vivo evaluation of a Tc-99m/99-dadt-benzovesamicol — a potential marker for cholinergic neurons. Nucl Med Biol 1994;21:197–203.

[24] Ding YS, Lin KS, Logan J, Benveniste H, Carter P. Comparative evaluation of positron emission tomography radiotracers for imaging the norepinephrine transporter: (S,S) and (R,R) enantiomers of reboxetine analogs ([C-11]methylreboxetine, 3-Cl-[C-11]

methylreboxetine and [F-18]fluororeboxetine), (R)-[C-11]nisoxetine, [C-11]oxaprotiline and [C-11]lortalamine. J Neurochem 2005;94: 337–51.

[25] Wouters W, de Coster R, van Dun J, Krekels MDWG, Dillen A, Raeymaekers A, et al. Comparative effects of the aromatase inhibitor R76713 and of its enantiomers R83839 and R83842 on steroid biosynthesis in vitro and in vivo. J Steroid Biochem Mol Biol 1990;37: 1049–54.

[26] Kopanska K, Najda A, Zebrowska J, Chomicz L, Piekarczyk J, Myjak P, et al. Synthesis and activity of 1*H*-benzimidazole and 1H-benzotriazole derivatives as inhibitors of *Acanthamoeba castellanii*. Bioorgan Med Chem 2004;12:2617–24.

[27] Carta A, Piras S, Boatto G, Paglietti G. 1*H*,6*H*-triazolo[4,5-*e*] benzotriazole-3-oxides and 5,5 '-(*Z*)diazene-1,2-diylbis(2-methyl-2*H*-1,2,3-benzotriazole) derived from chloronitrobenzotriazoles and hydrazine. Heterocycles 2005;65:2471–81.

[28] Wouters W, Decoster R, Tuman RW, Bowden CR, Bruynseels J, Vanderpas H, et al. Aromatase inhibition by R-76713 -— experimental and clinical-pharmacology. J Steroid Biochem Mol Biol 1989;34: 427–30.